APPLICATION OF FINITE ELEMENT METHODS TO THE ANALYSIS OF MAGNETIC CONTAMINATION AROUND ELECTRONICS IN MAGNETIC SENSOR DEVICES

Marina Díaz-Michelena [(1)], Ana Belén Fernández[(1)], Marco Maicas [(2)]

[(1)] INTA, Ctra Torrejón-Ajalvir km 4, 28850 Torrejón de Ardoz, Spain, Email: diazma@inta.es
[(2)] ISOM-UPM, Avda. Complutense 30, 28040 Madrid, Spain, Email: maicas@fis.upm.es

ABSTRACT

The number of missions devoted to the measurement of the magnetic field has dramatically decreased since the 80s, being the decrease in number accompanied by a reduction in the mass and economic budget of many of the exploration missions. This scenario was the seed for a new generation of sensors: the Commercial Off-The-Shelf (COTS) based microsensors. In the particular case of magnetometers, these miniaturized and compact devices imported a traditional problem of geomagnetic missions: the magnetic cleanliness trouble. Magnetic cleanliness, which is isolated in the platform when the magnetometer is deployed in a boom, becomes a real trouble when it has to be considered at Printed Circuit Board (PCB) level. In this work we present the description, method and results of a finite elements model for an engineering prototype of a NANOSAT-01 two axis magnetic sensor, launched in 2004. The idea is to extrapolate this method for all subsystems of a satellite.

1. INTRODUCTION

Magnetism constitutes one of the most interesting phenomena to be studied by space missions devoted to planetary exploration. Particular areas of interest are, for example, the magnetic shielding of the planets, which constitutes a key factor for life. Other area of interest is the analysis of the planet subsoil as the local magnetic fields can provide information about the constituent minerals. In these and other applications it is necessary to measure low magnetic fields so the development of new sensitive sensors is a major goal [1].

Unfortunately, magnetic measurements of low fields are affected by the magnetic contamination produced by the electronics associated to the sensor itself and the other equipment in the spacecraft or satellite. Therefore Magnetic Cleanliness Programs (MCP) need to be implemented in the spacecrafts with on board scientific magnetometers, to identify the main sources of magnetic fields and to know how these magnetic fields decrease with the distance [2]. MCP experimented a great progress in the decade of the 70´s, after Mariners with the deployment of the magnetometers on a boom (which requires the development of mechanical devices) and secondly with the dual technique [3]. Along the next decades, missions like Voyager and Ulysses implemented very good MCP with Cluster mission as the maximum example of this improvement [4]. However, MCP are very costly and difficult to implement, and nowadays only some of the missions can afford a magnetically "spick and span" spacecraft as it is the Kaguya-Selene case. (Fig.1)

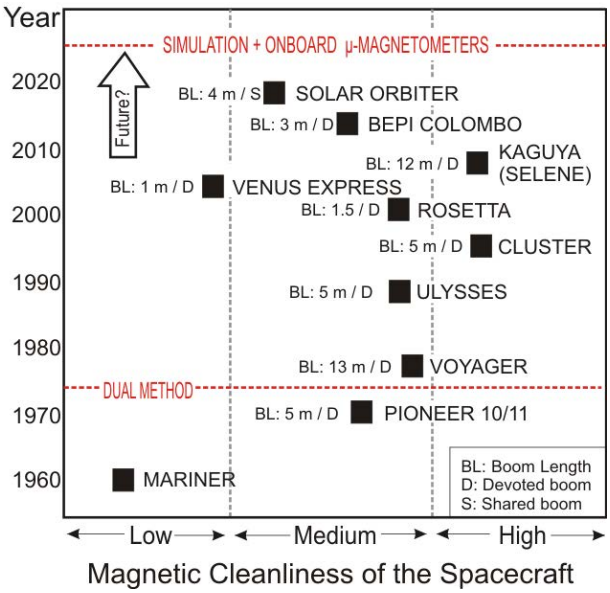

Figure 1. Authors view of MCP along the space exploration.

This paper addresses the development of a model to identify the main sources of magnetic fields and to understand the effects of the tracks in printed circuit boards (PCB), of some components (like inductors) and the magnetic materials (like transformer nuclei) in the spacecraft. This method allows implementing design solutions to achieve magnetic cleanliness at PCB level and improve sensor performances. However, the large number of tracks in a board, the components and their geometry makes mathematical models become very complex [5].

Numerical models can be considered for this task. Finite Element Methods (F.E.M.) are very useful when geometry constitutes a key point. The evaluation of the magnetic field can be made from currents in the board and components with magnetic properties, taking into account their location and geometry. A description of

the board considering these sources can provide an estimation of the field around the PCB and so their contribution to magnetic contamination. In this work we show the magnetic fields obtained by a FEM simulation around an electronic setup: NANOSAT-01 EM magnetometer, and their sensitivity with respect to the different magnetic sources. We also comment on the importance of these kinds of considerations when designing PCBs.

2. METHOD DESCRIPTION

Authors have used a PCB of NANOSAT-01 for the proposed method demonstration. NANOSAT-01 is the first nanosatellite of NANOSAT program of INTA, an initiative to validate in orbit new microtechnologies and nanoscience experiments. Thus, NANOSAT-01 had several microtechnology based sensors onboard: an AMR COTS four axis magnetometer, a set of solar sensors based on nanoporous Silicon, a magnetic sensor based on the Faraday effect of a Silica matrix with immersed γ-ferrite nanoparticles, as well a new technological experiment of wireless links with diffuse light.

F.E.M. calculation is performed on an EM of an AMR miniaturized sensor for NANOSAT-01. The objective is to combine PSPICE electronic simulation and F.E.M. simulation for the currents and magnetic fields intensities respectively in the early stages of the design to estimate the real operational conditions of the sensor and study how this situation matches the specifications of the sensor.

The simulations are compared with real measurements on a PCB to validate the results.

Authors have chosen this example: the EM magnetic sensor of NANOSAT-01 because it is a compact sensor with transducer (AMR COTS HMC1022 by Honeywell) and the front end electronics all integrated in the same PCB.

The PCB front end can be considered into 5 main groups: the two magnetic components: x and y conditioning electronics, the set-reset circuitry, the temperature compensation circuitry and the calibration circuit.

Prior to the simulations an exhaustive of magnetic characterization has been performed to the different electronic components of the part list of the sensor. Magnetic characterization implies to measure a hysteresis loop up to a magnetizing field of 2 T in the three different axes of the components to find the easy axis of magnetization, i.e. the axis on which magnetization tends to be. During the design stages it is recommendable that magnetic easy axes of components are not aligned with the transducer to reduce, at least by a factor of two, their magnetic signature at the position of the transducer.

The information of the magnetization versus magnetic field, ie M-H loops is used to create new libraries of magnetic components for the F.E.M. simulation. It has to be taken into account that electronic components are assimilated to hard magnetic materials with their remanence after the application of a moderate to high magnetic field of 2 T (worst case).

Values measured with the Vibrating Sample Magnetometer (VSM) of the coercive field and remanent magnetization of those electronic components with highest remanence are shown in Tab. 1.

Table 1. Table of coercive field and remanent magnetization of significant electronic components: instrumentation amplifier, logic gate, zener diode and the electrolytic capacitors.
Note that 1 A/m = $4\pi \cdot 10^{-3}$ Oe, 1 T = $10^4/4\pi$ emu/cm^3.

	X axis		Y axis		Z axis	
Component	**H_c (A/m)**	**$\mu_0 M_r$ (T)**	**H_c (A/m)**	**$\mu_0 M_r$ (T)**	**H_c (A/m)**	**$\mu_0 M_r$ (T)**
Instr. Amp.	$8{,}76 \cdot 10^3$	$1{,}23 \cdot 10^{-3}$	$1{,}15 \cdot 10^4$	$3{,}80 \cdot 10^{-3}$	$1{,}27 \cdot 10^4$	$1{,}26 \cdot 10^{-4}$
Logic Gate	$8{,}96 \cdot 10^3$	$8{,}56 \cdot 10^{-5}$	$1{,}16 \cdot 10^4$	$9{,}82 \cdot 10^{-5}$	$1{,}23 \cdot 10^4$	$7{,}60 \cdot 10^{-5}$
Zener	$1{,}20 \cdot 10^3$	$4{,}91 \cdot 10^{-3}$	$5{,}35 \cdot 10^2$	$2{,}44 \cdot 10^{-2}$	$1{,}20 \cdot 10^3$	$4{,}91 \cdot 10^{-3}$
Capacitor	$7{,}27 \cdot 10^3$	$2{,}91 \cdot 10^{-5}$	$6{,}78 \cdot 10^3$	$3{,}21 \cdot 10^{-5}$	$1{,}15 \cdot 10^4$	$3{,}43 \cdot 10^{-5}$

2.1. PSPICE Simulation

The PCB (Fig. 2 & 3) has been simulated with PSPICE. When PSPICE models were not available, some components have been modelled with an equivalent one (in terms of functionality and package) among the available libraries.

Two different profiles have been designed for the simulations: one devoted to a static calculation and another one for transient currents.

Results of the static simulation present nominal currents values in the order of 0.1 mA or much lower in almost all lines with the exception of some electrical lines, eventually close to the transducer, with currents in the order of several mA. In our model we have considered the lines with currents higher than 1 mA and some small loops that might cause a noticeable field by the transducer.

In the transient simulation special attention has been paid to the set-reset electrical current with intensities up to half of an Ampere. The design of the PCB is such that these current peaks are demanded from the accumulated charge of a couple of 10 μF capacitors, and thus not drawn from the power line. Therefore the peaks have been taken into account just locally in the proximity of the line and not in a global scale in the PCB.

2.1. F.E.M. Simulation

Magnetic fields around PCB have been modelled using Amperes Simulator (by ©Integrated Engineering

Software). We have selected the Boundary Elements Method (BEM) [6] to evaluate magnetic fields produced by the tracks carrying higher currents (I > 1 mA) and the electronic components that exhibit higher remanent magnetization (see Tab. 1). In order to compare simulation results with real sensor measurements we have magnetized electronic components in each of the three perpendicular directions and have developed models for all of them. These models consider the total magnetic moment for each component in the remanence state, measured previously by VSM, and the orientation of magnetization. Measured coercive fields in electronic components were much higher than magnetic fields in the PCB so magnetization in a single component is not expected to be altered by others. The tracks in PCB were modelled as current lines following the topology on the PCB. Simulations reported magnetic fields in the board and in the sensor location.

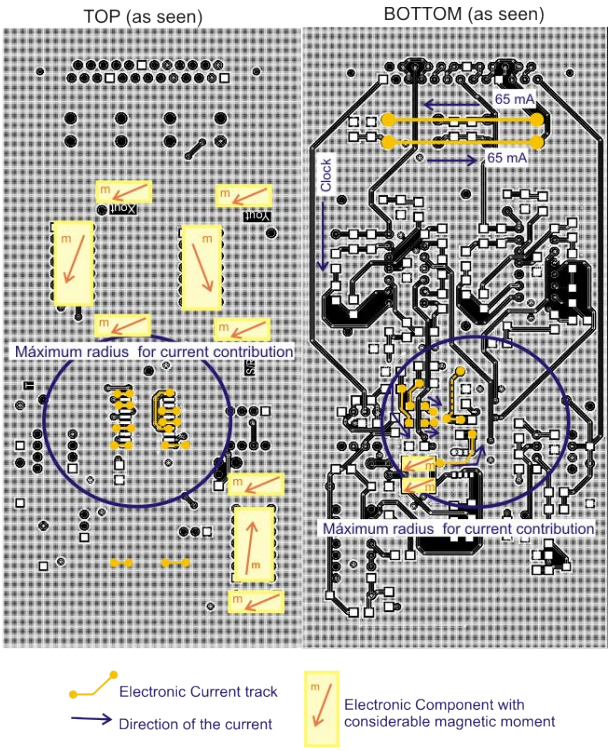

Figure 2. Top and bottom view of the magnetic sensor PCB showing the electronic components with considerable magnetic moment

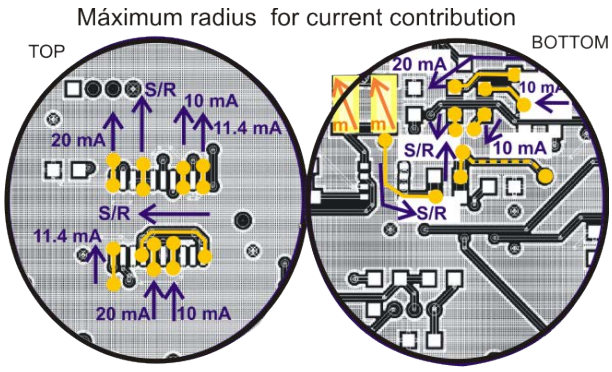

Figure 3. Zoom in of the area in which electrical currents are considered for the simulation. Notice that it is rotated and angle of 90 º respect to figure 2.

2.1. Magnetic field measurements

Magnetic field measurements in the PCB have been performed to check the results obtained with the simulations.

To do so in a controlled magnetic environment, the PCB was centred and fixed in a shielding chamber of CO-NETIC AA alloy (Magnetic Shield Corp., USA) which attenuates the external magnetic field in a factor of 10^4. The size of the chamber is much higher than that of the PCB, so as to not be affected by the shielding alloy contribution. The variation of the room temperature during the test was lower than 0.5 ºC.

A magnetic circuit has been used to magnetize the electronic components to apply a moderate to high magnetic field (between 30 and 50 mT) very localized in the position of the electronic component. Only the electronic components with higher remanence: the instrumentation amplifiers, the electrolytic capacitors, zener diodes, coils and a logic gate, have been magnetized alternatively in the positive and negative direction in every axis approaching the magnetic circuit to the PCB in such a way that the component is placed in the centre of the magnetic circuit air gap.

One question under discussion was the possible change in magnetization of the electrolytic capacitors with the high and nearby electrical current of the set and reset pulses: up to 0.5 A during 2 µs (enough to magnetize the components). However the estimated value of the magnetic field produced by the current (120 µT) is much lower than the coercive field of the electrolytic capacitors and thus the effect of this current in the capacitors magnetization is neglected.

The changes in the local field as a consequence of the different states of magnetization have been measured by means of the magnetic sensor HMC1002 by Honeywell. This sensor is a two axes one being the two axes designated by “A” and “B”. Its sensitivity is 3.2 mV/G (32 µV/µT), and per voltage of the Wheatstone bridge supply voltage. The measurements were performed with set and reset. So as not to affect the temperature of the

sensor during the measurement with the set and reset current pulses, the set reset was perform manually (not by means of a clock) respecting a temperature relaxation time after the pulses. This is possible since the PCB is in the centre of the shielding chamber and no appreciable change in the magnetic field is expected.

3. RESULTS

Both simulations and experiment have been devoted to magnetize the electronic components in both directions of every axes and see the differences between the two cases in the three axes with the two perpendicular transducers of the sensor.

F.E.M. simulation results and measurements show that differences in the magnetic field environment in the area of the sensor are of the order of 100's nT.

Tab. 2 shows magnetic field differences between positive and negative magnetizations: on the first hand measured with the sensors A and B (B_x and B_y respectively) and on the other hand performed with the F.E.M. simulation in the centre of the magnetic sensor.

Table 2. Variation of the magnetic field components ΔB_x, ΔB_y, ΔB_z when magnetizing in opposed directions measured with the sensor and simulated.

Magnetization direction	Measurements		Simulations		
	ΔB_x (μT)	ΔB_y (μT)	ΔB_x (μT)	ΔB_y (μT)	ΔB_z (μT)
X	0,20	0,32	2,95	0,59	0,53
Y	0,56	0,24	0,83	0,86	0,65
Z	0,26	0,10	0,58	0,49	0,14

Note that simulations have been performed for the three axes though the experiment could only be performed for the two axes corresponding to the sensing directions of the HMC1002.

It can be seen that the order of magnitude in the measurements and simulations is the same except in the case of the B_x component when magnetizing in the X direction.

Discrepancies of values are considered acceptable and actually could be helpful to determine the position of the A and B sensing AMRs in the HMC1002 since a certain field gradient is obtained in the volume of the sensor.

The results are considered successful and some discussion will be performed to explain the difference in values between measurements and simulations in the case of X axis magnetization below.

In the present case it has been observed that generally remanent magnetization of electronic components is dominant above the mA currents in the PCB.

For magnetization in the X direction (Fig. 4) it can be seen that the effect of the operational amplifiers (OA) is dominant in the simulation, generating a magnetic field B_x in the position of the sensor, only perturbed by the effect of the capacitors underneath the sensor, and the zener diodes located between the OAs and the sensor.

Actually, due to this predominancy the area between the two OAs is a region of high field gradient with considerable rotation of the field.

In order to explain the difference in order of magnitude of the B_x component of the field obtained with the different methods: measured and simulated, an extra simulation without OAs has been performed (Fig. 5).

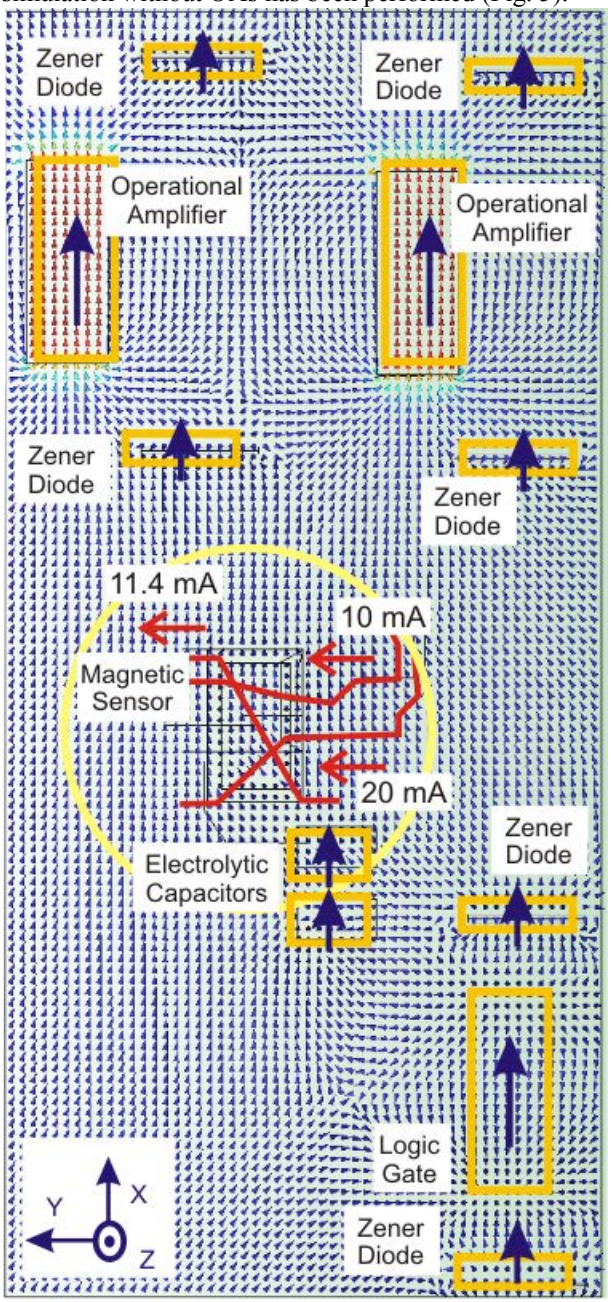

Figure 4. Simulation of the PCB when electronic components are magnetized in the X direction.

This simulation predicts almost no difference in the values of the calculated fields when magnetizing in Y and Z directions and very little incidence in the B_y and B_z components when magnetizing along the X direction.

However it plays a very important role in the B_x component when the electronic components are magnetized along X reducing the intensity of the field in one order of magnitude. In order to understand this, a the traceabiliy of the OAs has been analyzed. We found out that measured OA with the VSM has not been provided by the same manufacturer than the OAs soldered in the PCB. This fact can explain the changes obtained with direct measurements and simulations, since the alloys used in the different parts of the component as can be the pins, are not necessarily the same.

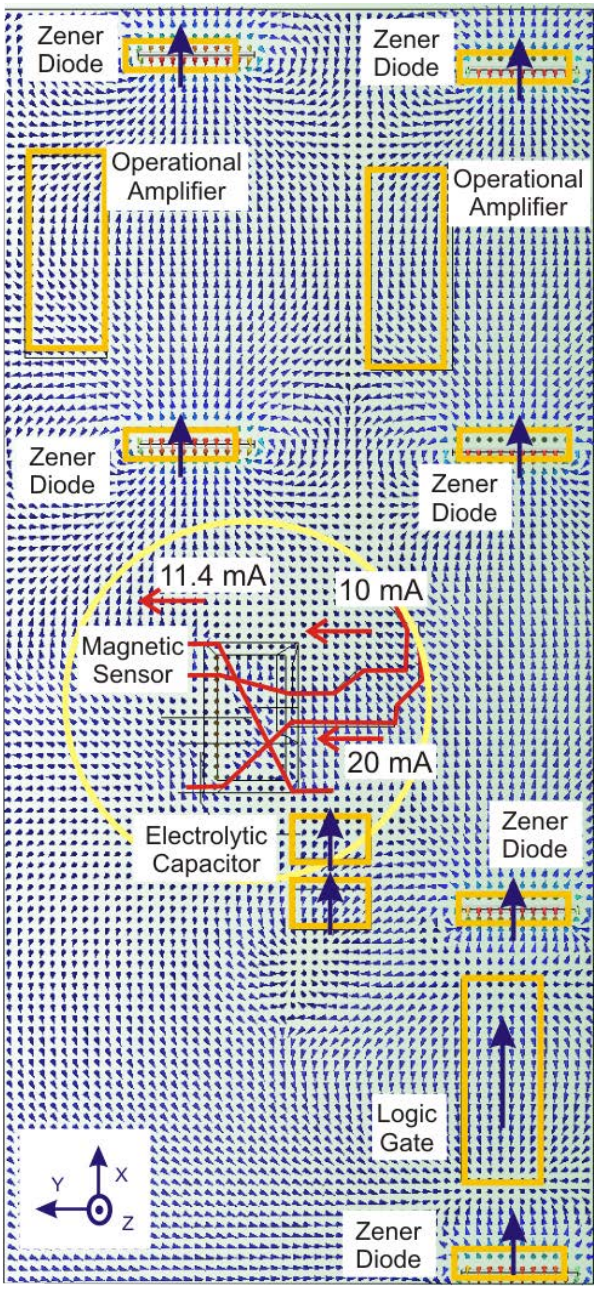

Figure 5. Simulation of the PCB when electronic components are magnetized in the X direction without the magnetization of the OAs.

Magnetization in the Y direction changes completely the situation giving rise to a weaker B_x in the position of the sensor and B^y component has opposed direction to that of the magnetization due to the fact that magnetic lines are closing in the area of the sensor. Change in sign is not reflect in Tab. 2 since values given in the table are in absolute value. In this case it is expected that currents have a value that can also be discarded since the approximate tracks in the area of the sensor are in the Y direction and thus induce a magnetic field in X and Z directions. As it has been commented, the higher values of the simulation respect to the measurements can be ascribed to the internal position of the A and B sensing elements in the AMR device.

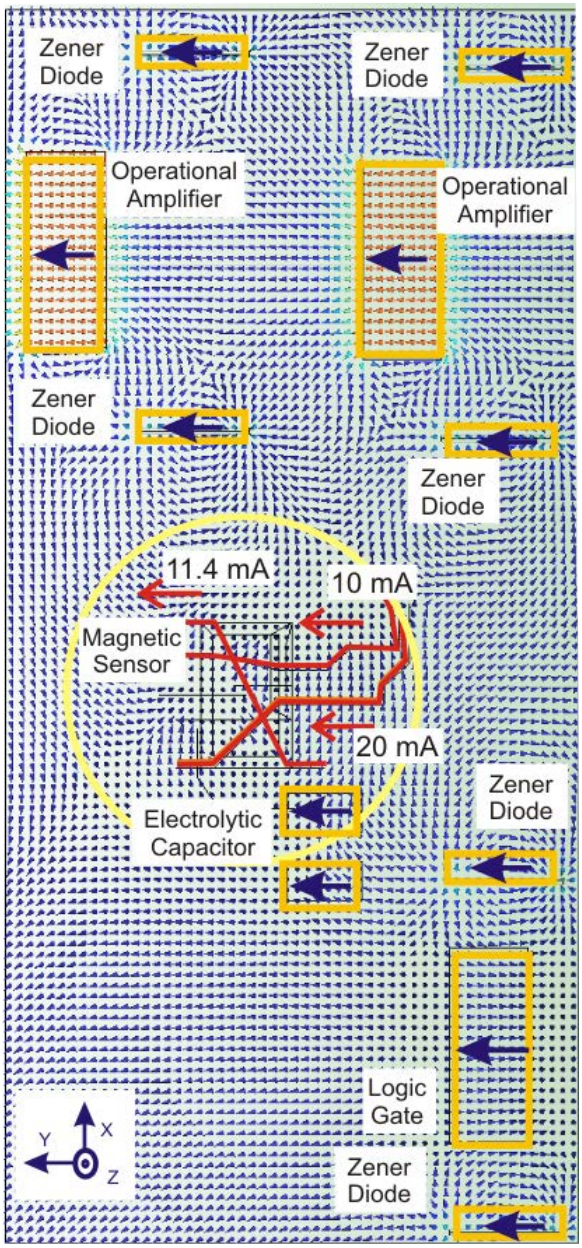

Figure 6. Simulation of the PCB when electronic components are magnetized in the Y direction.

Simulation has also been obtained with the magnetization in the Z direction (Fig. 6) even though no measurement has been performed in this axis due to the fact that the AMR sensor is a two axis magnetometer. In contrast with the other axes, in this simulation the electrical currents can have a relevant role in the surroundings of the sensor though this effect does not change the order of magnitude of the magnetic field simulated.

Simulated values have higher values than those measured but the order of magnitude corroborates that the evolution is compatible in both.

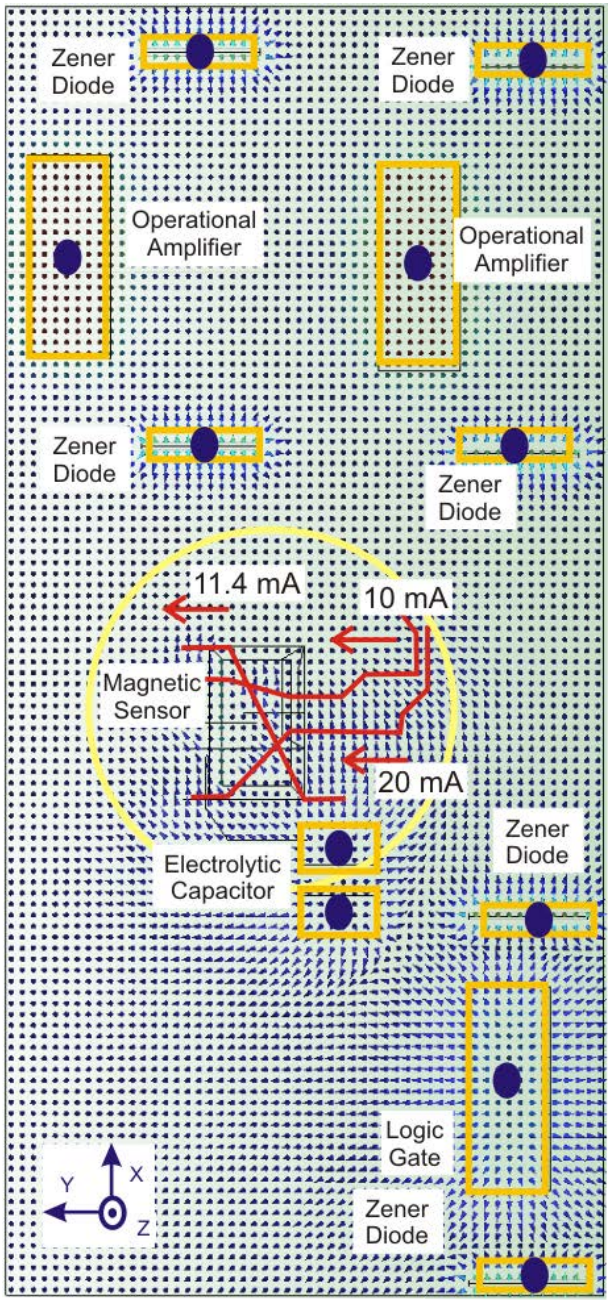

Figure 7. Simulation of the PCB when electronic components are magnetized in the Z direction.

4. CONCLUSIONS

An engineering model of a compact magnetic sensor has been used to demonstrate that combined electronic and finite element method simulation leads to calculation of representative magnetic fields in a mixed electronic and magnetic environment. This method makes it easier the design tasks in small magnetometers where magnetic cleanliness has to be implemented at printed circuit board level. The practice of this method permits the generation of a preferred part list of low magnetic moment electronic components as well as good practices in the electronics design.

The exercise can be extrapolated to the engineering and structural models of a spacecraft in a very initial stage of the mission development to detect the critical elements and reduce their magnetic signature in later prototypes.

5. REFERENCES

1. M.H.Acuña, (2002). Space-based magnetometers, Review of Scientific Instruments **73** (11), 3717

2. K. Mehlem, A. Wiegand, Magnetostatic Cleanliness of a Spacecraft, (2010). 2010 Asia-Pacific International Symposium on Electromagnetic Compatibility, April 12 - 16, 2010, Beijing, China

3. Ness, N. F., K. W. Behannon, R. P. Lepping and K. H. Schatten, (1971) Use of two Magnetometers for Magnetic Field Measurements on a Spacecraft, Journal of Geophysical Research, **76**, 3565-3573, 1971

4. A. Balogh *et al.*, (1993). The Cluster Magnetic Field Investigation: Scientific Objectives and Instrumentation, ESA SP-1159, 96-114

5. K. Mehlem, (1978). Multiple magnetic dipole modeling and field prediction of satellites, IEEE Transactions on Magnetics **14** (5), 1064-1071, ISSN: 0018-946

6. Y.B. Yildir *et al.*, (1991). Three dimensional analysis of magnetic fields using the boundary element method, Integrated Engineering Software, ww.in-tegratedsoft.com/papers/techdocs/tech_1ax.pdf

6. ACKNOWLEDGEMENTS

This work has been partially supported by the Spanish Nacional Program of R&D externalization via the projects of references PRI-PIBUS-2011-1150 and PRI-PIBUS-2011-1182. Ana Belén Fernández acknowledges INTA for the scholarship she enjoys.

Authors acknowledge Prof. Claudio Aroca for his help with the magnetizing magnetic circuit design.